Limnological Dynamics and Phosphorus Budget Analysis for Lake Desair, Wisconsin

Northwest Creek flow gauging equipment, 2013

25 November, 2013

William F. James
University of Wisconsin – Stout
Discovery Center - Sustainability Sciences Institute
Menomonie, WI 54751
715-338-4395
williamfjames@charter.net
jamesw@uwstout.edu

EXECUTIVE SUMMARY

Lake Desair currently exhibits eutrophic to hypereutrophic conditions (Carlson TSI = 62 to 67) with a summer average total phosphorus (P), chlorophyll, and Secchi transparency of 0.078 mg/L, 56 µg/L, and 0.9 m, respectively. A monitoring program was conducted in 2013 to examine seasonal lake P and chlorophyll dynamics in relation to internal and tributary P loading and to predict changes in these variables as a function of reduction in P loading. P loading from Northwest (NW) Creek was greatest in late March and early April in conjunction with snowmelt. Frequent precipitation events in April through June also resulted in elevated P loading. Annual total P loading was estimated at 755 kg/y and SRP, which is more directly available for algal uptake, represented nearly 40% of the NW Creek input to Lake Desair.

The lake was strongly stratified between late May and October with development of hypolimnetic anoxia that extended up to the 4-m depth. The anoxic factor (i.e., days that a sediment area normalized with respect to the lake surface area is anoxic) was high at ~ 95 d. Both iron (Fe) and P (primarily in soluble form) increased substantially in the anoxic hypolimnion throughout the summer. Internal P loading, estimated by mass balance, was high at ~ 350 kg/y or ~ 10 mg/m^2 d and accounted for 32% of the measured annual P loading contribution to the lake. No physical entrainment of soluble P into the epilimnion for potential uptake by algae was detected during the summer stratified period or fall turnover. This apparent lack of vertical upward transport was due to a high Fe:P ratio in the anoxic hypolimnion, which resulted in complete precipitation and adsorption of P during chemical oxidation rather than algal uptake. Thus, hypolimnetic P availability via lake mixing was controlled by Fe oxidation-reduction reactions. Vertical profiles of chlorophyll indicated that peaks (unknown species) of either algae or perhaps chemosynthetic bacteria occurred in the upper hypolimnion in the vicinity of high hypolimnetic P gradients. These preliminary observations need to be explored in greater detail in 2014 to determine if biological P assimilation by motile algae is occurring in the

lake. If so, these algae may be accessing hypolimnetic P gradients for assimilation and growth in August.

Steady-state empirical modeling suggested that controlling soluble P loading in the NW Creek subwatershed will be needed to improve summer water quality conditions in Lake Desair. For instance, a 50% reduction in NW Creek P loading would result in a predicted decline in lake total P from ~ 0.078 mg/L to 0.059 mg/L. Chlorophyll would decline by ~ 43% to 31 µg/L and Secchi transparency would increase from a mean 0.9 m to a predicted 1.2 m.

RECOMMENDATIONS

1. Pursue the development and implementation of a Total Maximum Daily Load (TMDL) for phosphorus.
2. Conduct a detailed watershed survey that includes a phosphorus index evaluation (i.e., SnapPlus) and soil crop-available P to identify critical source and transport areas for management to reduce SRP loading from the NW Creek subwatershed.
3. More information is needed to better evaluate the potential effectiveness of artificial circulation/destratification in managing phytoplankton biomass. The phytoplankton assemblage and possibility of vertically migrating algal species should be examined in 2014 to determine the potential importance of direct access and assimilation of hypolimnetic P sources by motile algal species. Samples would need to be collected seasonally and at different depths for taxonomic identification. A series of in situ loggers with chlorophyll fluorescence probes (up to 4) should be deployed between the 1-m and 5-m depths in July and August to detect algal biomass peaks and movement in relation to the vertical P profile. A P profile should be collected once in July and once in August at a minimum for comparison with peaks in algal biomass in the water column.

OBJECTIVES

The objectives of this research were to examine seasonal lake P and chlorophyll dynamics in relation to internal and tributary P loading and use a predictive empirical steady-state model to explore the impacts of P loading reduction scenarios on average summer lake water quality conditions.

STUDY SITE

The 1,500 ha watershed draining into Lake Desair (Fig. 1) is characterized by steeply sloping topography and coulees that rapidly drain land uses dominated by row crop agriculture and forest areas (52% and 42%, respectively; Cedar Corporation 2006). The largest subwatershed draining into the lake, Northwest (NW) Creek, has the greatest agricultural land use at ~64% (Fig. 2).

Lake Desair, located near the City of Rice Lake, is relatively small (surface area = 32 ha; water volume = 1.6 m^3; mean depth = 5.1 m; maximum depth = 10.1 m) lake formed during the last ice age (Table 1). The lake is elongated along the northeast-southwest axis with a maximum fetch of ~1.3 km. Basin morphometry is approximately linear with increasing depth (Fig. 3). The Osgood Index for the lake is 9.0 (i.e., mean depth divided by the square root of the surface area). Lakes with values < 6 are more susceptible to wind-generated mixing. Historically, the lake is classified as eutrophic to hypereutrophic (TSI_{TP}=69; TSI_{chla}=67; TSI_{SD}=54) and mean summer surface concentrations (averaged over a 20 year period between 1993 and 2011) of total phosphorus (TP), chlorophyll, and Secchi disk transparency are 0.07 mg/L (range = .042 to .109 mg/L), 40 mg/m^3 (range = 12 to 140 mg/m^3), and 1.52 m (range = 0.98 to 1.97 m), respectively.

METHODS

Tributary Hydrology and Constituent Loading

A gauging station was established on NW Creek in the drainage culvert under 18th Ave between March and October, 2013. A data logger and area-velocity meter (ISCO Model 4150; Hach Co., Loveland, CO) collected velocity (m/s or ft/s) and stage height (m or ft) at 15-min intervals. Volumetric flow (Q, m^3/s or ft^3/s) was estimated from this information using ISCO Flowlink® 5 software.

Water grab samples were collected by volunteers during periods of flow between March and the end of June total phosphorus (TP) and soluble reactive phosphorus (SRP). Samples for SRP were filtered in the field through a 0.45 µm filter. Collected samples were frozen until analysis. Flow subsided at the end of June and the creek was essentially dry through October. Annual and seasonal phosphorus (P) loading (kg/y or kg/d) were estimated using the computer program FLUX (Walker 1996).

Limnological Monitoring

Water samples and in situ profiles were collected biweekly to monthly between late May and early November at a centrally-located station (Fig. 4). In situ vertical profiles of temperature, dissolved oxygen, specific conductance, and pH were measured using a Hydrolab Quanta® (Hach Co., Loveland, CO) that was precalibrated against known buffer solutions and Winkler dissolved oxygen analyses. Measurements were collected at 1-m intervals between the lake surface and within 0.2 m above the bottom (maximum average depth = 9 m). Water transparency was estimated using a 20-cm alternating black and white Secchi disk. Water samples were collected between 2 m and within 0.2 m above the bottom using a peristaltic pump and tubing and stored in a cooler on ice in the field. Additionally, an integrated sample was collected over the 1-m water column using a schedule 40 1.25 inch PVC pipe attached to a one-way valve. For dissolved constituent analysis, samples were pumped directly into a 60-cc syringe without exposure to air and filtered through a 0.45 µm filter. All samples were analyzed for TP, SRP, total iron (TFe), and dissolved iron (DFe). The integrated sample was also analyzed for viable chlorophyll a. Vertical profiles of chlorophyll were examined in August through November, 2013.

Schmidt stability (S; g-cm/cm^2) was calculated as:

$$S = 1/A\int_0^{z_m}(z - z_g)(\rho_z - \rho_g)dz \qquad 1)$$

where A = surface area (m^2), z_m = maximum depth (m), z = depth at stratum *z*, z_g = depth of the center of mass or ρ_g, and ρ_z = the density of water (kg/m^3) at depth *z* (Idso 1973). ρ_g was calculated as:

$$\rho_g = 1/V\int_0^{z_m} V_z \rho_z dz \qquad 2)$$

where V is lake volume (m^3) and V_z is the volume at depth z. Schmidt stability represented the amount of work (in the form of wind power, motor boat activity, etc) required to completely mix a water body that is stratified due to vertical differences in water density. Higher stability values were indicative of strong stratification and greater work required to disrupt stratification. Conversely, lower stability values were indicative of weak stratification and less work required to disrupt stratification.

Phosphorus Budget, Empirical Modeling, and Phosphorus Loading Reduction Scenarios

Summer P budget approaches were used to assess the importance of external and internal P sources to Lake Desair (expressed as kg; kg/summer; or kg/y). Annual internal P loading was estimated empirically using equations developed by Nürnberg (1998 and

2009). In addition, net internal P loading ($P_{net\ internal\ load}$) was defined as the flux of P from sediment stored in the lake in excess of P sedimentation. $P_{net\ internal\ load}$ was estimated by difference from the equation,

$$\Delta P_{lake\ storage} = (P_{external\ load} - P_{outflow}) \pm P_{net\ internal\ load} \qquad 3)$$

where $\Delta P_{lake\ storage}$ = the change in lake P mass over a defined summer period, $P_{external\ load}$ = the P mass input to the lake from NW Creek, and $P_{outflow}$ = the P mass that was discharged from the lake. $P_{lake\ storage}$ was calculated as,

$$P_{lakestorage} = \sum_{i=0}^{n} P_{concentration} \cdot Volume \qquad 4)$$

where $P_{concentration}$ = the TP concentration (mg/L or g/m^3) and Volume = the water volume (m^3) at depth *i* (m). The product of these variables (kg) for each depth layer was summed over the entire water column (n = maximum depth, m) to estimate $P_{lake\ storage}$. It was assumed that discharge from the lake was approximately equal to Q at NW Creek to estimate $P_{outflow}$. Mass estimates were converted to rates (mg/m^2 d) by dividing mass by the area of the lake and defined time period (~ 111 days).

The summer anoxic factor (AF, d/summer), days that a sediment area normalized with respect to the lake surface area is anoxic, was quantified for 2013 according to the following equation developed by Nürnberg (1995) as,

$$AF = \frac{\sum_{i=1}^{n} t_i a_i}{A_{LakeSurface}} \qquad 5),$$

where, t_i = the time interval of anoxic conditions (d), a_i = anoxic sediment area over the interval (m^2), and $A_{LakeSurface}$ = the lake surface area (m^2). Anoxia was defined as dissolved oxygen concentration less than or equal to 1.0 mg/L.

Empirical steady-state modeling and loading reduction scenarios were examined using *Bathtub* (Walker 1996). *Bathtub* is a windows-based software program that provides a suite of equations for predicting lake average P, chlorophyll, and Secchi transparency. Response of these variables to increases and decreases in P loading (external and internal) was used to evaluate management alternatives.

Analytical Methods

Samples for TP were predigested with potassium persulfate according to Ameel et al. (1993) before analysis. SRP samples were filtered through a 0.45 μm filter prior to analysis (Millipore MF). Phosphorus species were determined colorimetrically using the ascorbic acid method (APHA 2005). Samples for TFe were digested with nitric and hydrochloric acid according to EPA metals digestion method 3050b. TFe and DFe was analyzed using atomic absorption spectrophotometry (APHA 2005). Chlorophyll was determined via a fluorometric technique following extraction in a 1:1 solution of acetone and dimethyl sulfoxide (Welschmeyer 1994).

RESULTS AND DISCUSSION

Hydrology and tributary loading

Daily precipitation, measured at the Eau Claire, Wisconsin Airport, was above average in March through June, 2013, due to numerous storms than often exceeded an inch (Fig. 5). Daily precipitation subsided by the end of June and dry conditions predominated between July and mid-September. Smaller storms occurred at a more moderate frequency in late September through early November.

Discharge from the NW Creek subwatershed was greatest in late March-early April in conjunction with snowmelt and precipitation patterns (Fig. 5). Frequent discharge peaks occurred in April through May, then flows declined in May through early June even though storms were still frequent and daily precipitation often exceeded one inch. In particular, discharge peaks were much smaller in mid-May through mid-June even though daily precipitation peaks often exceeded one inch during this period. Establishment of cover crops and leaf formation in forested areas may have played a role in intercepting precipitation and reducing runoff. NW Creek discharges were undetectable after late June. Drought conditions, coupled with probable interception and complete infiltration of precipitation during these smaller lower intensity storms undoubtedly played an important role in minimal runoff. Overall, NW Creek areal water load was modest at 5.4 m/y and theoretical water residence time (i.e., the time to completely refill the lake with new water) for Lake Desair was relatively high at 0.9 y.

Concentrations of TP and SRP were greatest during the snowmelt period of late March through early April (Fig. 5). During this period, TP was very high, exceeding 1 mg/L (range = 0.410 to 1.117 mg/L). SRP in the discharge, which can be directly assimilated by algae for growth, was also very high, ranging between 0.176 and 0.361 mg/L, and represented between 22 to 55% of the TP. Concentrations of both constituents declined from these peaks during late April discharge events and then increased in conjunction with storm inflows occurring in late May and early June. This seasonal pattern may have been related to agricultural activities (i.e., field preparation and planting) in the NW Creek watershed.

The annual flow-weighted TP and SRP concentration were relatively high at 0.431 and 0.158 mg/L, respectively (Table 3), and SRP accounted for ~ 37% of the TP loading composition (Fig. 6). Most of this TP and SRP loading occurred during the spring (Fig. 5). In contrast, summer loads (i.e., June – September) were very modest at 19 and 5 kg for TP and SRP, respectively (Table 3). The annual TP export coefficient for NW Creek was moderately high at 0.74 kg P/ha y (0.66 lbs/ac y) and fell within the "most likely" range for watersheds with greater than 50 to 75% agricultural land use practices in Wisconsin (Panuska and Lillie 1995).

Limnological patterns in Lake Desair

Stratification patterns and iron-phosphorus dynamics. Lake Desair exhibited strong stratification patterns with high thermal stability (i.e., low mixing potential) in 2013 (Fig. 7). The lake gained heat rapidly between May and late July, resulting in the development of an epilimnetic mixed layer that was ~ 2 to 3 m in thickness (Fig. 8). An apparent cold front in late July resulted in temporary surface cooling and a slight decline in stability; however, stratification remained strong during this period and warmer air temperatures in August resulted in net heat gain. Hypolimnetic temperatures were very cool throughout the summer and only increased slightly between May and September (i.e., from 5.5 to 7 ^{o}C; Fig. 7). This pattern suggested that there was very little downward heat entrainment via mixing and that exchanges between the epilimnion and hypolimnion were minimal during the summer period. Air temperature cooling between September and November resulted in gradual epilimnetic expansion and thermocline erosion. The lake was completely mixed in early November.

Dissolved oxygen depletion and anoxic conditions developed rapidly in the hypolimnion in conjunction with stratification (Fig. 7). Bottom waters above the sediment-water interface were anoxic by early June and hypolimnetic anoxia extended up to near the 3-m depth by August. The anoxic factor (i.e., the number of days that an area equivalent to the lake surface area is anoxic) was high at ~ 95 d, falling within ranges observed for some other eutrophic lakes in the United States (Mendota, Onondaga, Rawson, Shagawa, E. and W. Twin; Nürnberg 1995).

Interestingly, dissolved oxygen concentrations declined substantially throughout the water column during the fall turnover period between late October and early November (Fig. 7). Concentrations ranged between only 4.2 and 4.5 mg/L throughout the water column (including the lake surface) during this period. As discussed further below, this pattern was related to chemical reaction of dissolved oxygen with high concentrations of DFe that had built up in the hypolimnion during the stratified period as a result of microbial reduction and diffusion out of the sediment.

TP and TFe concentrations increased substantially in the hypolimnion throughout the summer stratified period in conjunction with the development of anoxia (Fig. 9). By late September, TP exceeded 1.4 mg/L and TFe approached 9 mg/L above the sediment-water interface and strong concentration gradients extended up to the thermocline (Fig. 10). In addition, soluble P and Fe usually accounted for greater than 90% of the total composition (not shown). There was also a strong linear relationship between hypolimnetic Fe and P concentration (both total and soluble species; Fig. 11) and the overall Fe:P ratio exceeded 5:1. The fall turnover period resulted in disruption of hypolimnetic TP and TFe gradients and complete mixing, with subsequent uniform and relatively higher concentrations throughout the water column by early November (Fig. 9).

This pattern was consistent with the Mortimer (1941, 1942, 1971) model of Fe control of P cycling from sediment. In this scenario, iron oxyhydroxides (Fe~(OOH) bind phosphate (PO_4^{3-}) within the sediment oxidized microzone (i.e., thin oxygenated and aerobic surface sediment layer on the order of less than 1 mm), preventing its diffusion into the water column under aerobic conditions. Under anoxic conditions, microbial reduction of Fe~(OOH) to Fe^{2+} in the sediment surface layer results in desorption of PO_4^{3-} and diffusion of both Fe^{2+} (measured as DFe) and PO_4^{3-} (measured as SRP) into the hypolimnion over the summer stratified period. Mixing and reintroduction of dissolved oxygen during fall turnover results in chemical reaction and oxidation of Fe^{2+} to Fe~(OOH) colloids (i.e., very low molecular mass Fe~(OOH) polymers), precipitation or adsorption of PO_4^{3-}, and eventual deposition. Precipitated and adsorbed PO_4^{3-} is generally not directly available for algal assimilation.

I could not delineate the Fe and P species during fall turnover due to limitations in the analytical methodology. Specifically, differentiation of particulate and soluble Fe and P could not be determined using conventional filtration techniques (i.e., filtration through a 0.45 µm filter to separate particulate and soluble species) because low MW Fe~(OOH)-PO_4 colloids are small enough to pass though 0.1 µm pore size filter. Under these circumstances, adsorbed PO_4^{3-} is artificially detected as SRP (rather than particulate P) due to acidic reaction with molybdate during the analysis. However, research has shown that Fe~(OOH)- PO_4 formation is complete at Fe:P ratios of 3.6:1 or greater (Gunnars et al. 2002), resulting in minor to zero PO_4^{3-} availability for algal uptake during periods of hypolimnetic reoxygenation.

Surface chemistry, trophic state index, and algal dynamics. Surface-integrated (i.e., upper 1-m water column) TP and chlorophyll increased to a peak in mid- to late June following a period of elevated NW Creek P loading in May to mid-June (Fig. 12). In particular, surface-integrated chlorophyll concentrations increased substantially to greater than 150 µg/L in June while Secchi disk transparency declined to less than 1 m. Surface-integrated chlorophyll declined ~ 24 µg/L in July, then exhibited another peak between August and late September. Secchi disk transparency increased to nearly 1.5 m in July in conjunction with lower chlorophyll, then declined to less than 1 m during the second chlorophyll concentration peak. Chlorophyll concentrations declined substantially during the fall turnover period, resulting in increased Secchi disk transparency (i.e., peak = 2.0 m). In contrast, surface-integrated total P concentrations increased substantially during the fall turnover period. This pattern was unrelated to chlorophyll biomass production and, instead, occurred as an apparent result of the formation of Fe~(OOH)-PO_4 complexes, as discussed above.

Mean summer (May – September) concentrations of TP and chlorophyll were very high at 0.078 mg/L and 56 µg/L, respectively, while mean Secchi disk transparency was only 0.9 m (Table 4). The mean Carlson Trophic State Index ranged between 62 and 67, indicative of highly eutrophic to hypereutrophic conditions.

Vertical profiles of chlorophyll revealed the unusual occurrence of concentration peaks located at the top of the hypolimnion in August and September (Fig. 13). These peaks were positioned in anoxic water well below the euphotic zone and in the vicinity of relatively high hypolimnetic SRP concentrations. Although these observations are notable, more information is needed in order to clarify the type of organism or community residing at these depths. For instance, they may be chemosynthetic algae or bacteria versus photosynthetic algae. In addition, taxonomic identification will be useful in shedding light on the possibility of vertical migration by algal into the hypolimnion for direct access and assimilation of P for growth. Several algal species are equipped with flagella or gas vacuoles and can actively migrate on a diel basis.

Summer and Annual Phosphorus Budget Analysis

The time period used for estimating $P_{net\ internal\ loading}$ was based on the net increase in $P_{lake\ storage}$ between an early summer minimum (i.e., near the onset of stratification) in late May and a maximum P mass that occurred near the onset of fall turnover in early September (Fig. 14). $P_{lake\ storage}$ mass exhibited a net increase of ~ 360 kg during this period (Table 5). $P_{external\ load}$ was very low during this period, indicating that $P_{net\ internal\ load}$ (solved by difference using equation 4) was the overwhelmingly dominant P source to the lake (Table 5). As discussed above, this net internal P load was confined to the hypolimnion due to strong stratification, lack of entrainment, and control of P by Fe in the oxidized state.

The area-based $P_{net\ internal\ load}$ was relatively high 9.8 mg/m^2 d. This rate compared well with independently-estimated rates of internal P loading (Table 6). For instance, the mean rate of P release from sediment determined independently from intact sediment cores (estimate 3 in Table 6) was very similar to the net internal P loading rate estimated via mass balance. On an annual basis, estimated internal P loading accounted for 32% while NW Creek loading represented ~ 68% of the measured annual P inputs to the lake (Fig. 16).

Annual Steady-State Empirical Modeling

Empirical models used in the Bathtub annual projections are shown in Table 7. I used the mean epilimnetic values shown in Table 4 to calibrate the model and assumed that both NW Creek P loading and internal P loading entrained into the epilimnion could impact surface-integrated lake TP concentrations. For initial runs, I included annual external P loading inputs from NW Creek only to predict lake TP (i.e., internal P loading was not included). Overall, the model slightly overestimated mean lake TP by ~ 9 μg/L (Fig. 17). This result suggested that watershed P loads (i.e., primarily from NW Creek), rather than internal P loading, were primarily responsible for the high surface-integrated mean TP concentration in the lake (i.e., incorporation of internal P loading would have resulted in further overestimation of mean lake TP) . This finding was corroborated by several lines of evidence – 1) even though internal P loading was relatively high in Lake Desair, the occurrence of dissolved Fe and the high Fe:P ratio in the hypolimnion resulted in precipitation of P from the water column rather than entrainment into the surface waters as available PO_4^{3-}, 2) surface-integrated chlorophyll concentrations were maximal in June in conjunction with periods of elevated NW Creek P loading in May and June, 3) NW Creek SRP loading was also significant during these periods and directly available for algal assimilation, and 4) surface-integrated chlorophyll concentrations declined during the fall turnover period, rather than increasing, further suggesting that internal P loads were being precipitated versus directly available for assimilation. This initial model setup also closely predicted mean surface-integrated chlorophyll and Secchi disk transparency (Fig. 17).

Model output suggested that substantial reductions in NW Creek P loading might be needed to improve lake limnological conditions (Fig. 17; Table 8). For instance, a 50% reduction in annual NW Creek P loading through best management practices (BMP) implementation would result in a predicted ~ 32% decrease in the mean annual lake TP concentration to ~ 0.060 mg/L. Predicted chlorophyll would be expected to decline to ~ 31 μg/L (a 43% improvement over the current mean) and Secchi disk transparency would increase to 1.2 m (a 32% increase over the current mean) under these loading reduction conditions.

Predicted bloom frequency (i.e., percentage of time in the summer that chlorophyll concentration exceeds a given value) would also improve with substantial reduction in NW Creek P loading (Fig. 18). For instance, algal blooms exceeding ~ 30 µg/L (i.e., a level at which lake users begin to notice a visible nuisance problem) currently occur about 75% of the time during the summer. A 50% reduction in NW Creek P loading would result in a predicted frequency of occurrence of only ~ 40% of the time (Table 9).

CONCLUSIONS AND MANAGEMENT IMPLICATIONS

Although summer internal P loading from anoxic sediment was high, it did not appear that physical mixing, vertical water exchanges, and entrainment of PO_4^{3-} into the well oxygenated epilimnion was directly important in fueling algal blooms in Lake Desair. Rather, the high Fe:P ratio in the hypolimnion strongly indicated that Fe oxidation and reduction processes were regulating SRP, and essentially trapping it in the hypolimnion and sediment (Gunnars et al. 2002). Termed the *ferrous wheel* (Campbell and Torgersen 1980), PO_4^{3-} adsorbed or precipitated onto Fe~(OOH) is retained in the sediment oxidized microzone. Depletion of dissolved oxygen at the sediment-water interface forces microbial anaerobic metabolism and reduction of Fe~(OOH) to Fe^{2+}. This metabolic transformation results in desorption of P and diffusion of both constituents (i.e., Fe^{2+} and PO_4^{3-}) out of the sediment and into the anoxic hypolimnion during summer stratification. Although concentration increase can be substantial in the hypolimnion over the summer stratified period, reintroduction of dissolved oxygen during periods of wind-generated epilimnetic expansion and turnover drives chemical oxidation of Fe^{2+} to Fe~(OOH) and reaction with PO_4^{3-} (Mayer et al. 1982). Since chemical oxidation and hydrolysis of Fe^{2+} is generally rapid, on the order of hours to a day (Davison 1993; Gunnars et al. 2002), most of the PO_4^{3-} becomes either adsorbed (Gunnars et al. 2002) or precipitated (Gunnars and Blomqvist 1997) and eventually returns back to the sediment rather than becoming assimilated by algae.

An important aspect of coupled Fe-P redox reactions is the stoichiometric relationship between Fe and P in the hypolimnion. Generally, complete P scavenging by Fe~(OOH) occurs when the Fe:P ratio is greater than 3.6:1 on a mass basis (2:1 on a molar basis; Gunnars et al. 2002). The overall hypolimnetic Fe:P ratio in Lake Desair approached 6:1 throughout the summer stratified period (Fig. 11), indicating coupled Fe-P interactions with complete adsorption or precipitation of PO_4^{3-} and return to the sediment during reoxygenation instead of incomplete scavenging and entrainment of PO_4^{3-} into the epilimnion for algal uptake. Chlorophyll concentrations declined during the fall turnover period in Lake Desair, lending further support to the role of the ferrous wheel in controlling hypolimnetic PO_4^{3-}. In contrast, Cedar Lake (Star Prairie, WI) experiences a similarly high internal P loading rate but the Fe:P ratio in the hypolimnion is less than 1:1. During fall turnover in this lake, high PO_4^{-} availability as a result of inefficient P binding generates massive algal blooms into October and early November.

Water column total Fe and P concentrations were very high for an extended period of time during fall turnover and actually reached a peak in early November in conjunction with substantial declines in surface dissolved oxygen, due to chemical oxidation (i.e., chemical consumption of dissolved oxygen by Fe; Fig. 12). These patterns were probably related to the formation of low molecular mass colloidal Fe~(OOH) complexes that can occur at the nanoparticle scale (i.e., as small at 1 nm; Hens and Merckx 2002; Thibault et al. 2009) and, thus, remain suspended in the water column. At these small scales, settling velocities and flux back to the sediment will likely be a slow process. Additionally, some colloidal Fe~(OOH)- PO_4 could be also exported via discharge from the lake.

At this point, relatively high Fe appears to be controlling internal P loading in Lake Desair. However, future decreases in the Fe:P ratio and decoupling of Fe-P linkages are possible if sulfate loading were to increase to a point where its microbial reduction in the hypolimnetic sediment removes Fe from further recycling via formation of iron sulfide

(FeS_x; Caraco et al. 1989, 1993; Roden and Edmonds 1997; Hupfer and Lewandowski 2008; Hoffman et al. 2013). Under these circumstances, both Fe^{+3} and Fe^{+2} compounds can be diagenetically reduced to FeS_x (Golterman 1984, 2001; Miltenberg and Golterman 1988; Amirbahman et al. 2003) as,

$$2Fe\sim(OOH) + 3HS^{-} = 2FeS + S + 3OH^{-} + H_2O \qquad 6)$$

and,

$$Fe^{-2} + HS^{-} = FeS + H^{+} \qquad 7).$$

Sulfide can also react with the mineral vivianite ($Fe_3(PO_4)_2 \cdot 8H_2O$) after depletion of siderite ($FeCO_3$) according to the equilibrium equation,

$$Fe_3(PO_4)_2 \cdot 8H_2O + 3H_2S = 3FeS + 2H_3PO_4 + 8H_2O \qquad 8),$$

to form FeS_x, leading to an uncoupling of the Fe-P association as iron becomes depleted from reaction with P through FeS_x formation. Generally, S becomes a factor in P recycling when the Fe:S ratio declines below 1. Coprecipitation or chelation between Fe and organic matter can also lead to burial of Fe and removal from the *ferrous wheel* (LaLonde et al. 2012; Kleeburg et al. 2013). Although not measured or examined during this present study, it does not appear that S or organic matter reactions with Fe are important controlling mechanisms in Lake Desair.

Empirical modeling suggested that P loading from NW Creek was primarily responsible for stimulating the occurrence of nuisance algal blooms in Lake Desair. In particular, SRP concentrations and loads were relatively high during storm inflows, and much of this fraction is probably directly available for algal assimilation. Even though most of the NW Creek P loading occurred in conjunction with snowmelt in late March and early April, the relatively long water residence time and, thus, P storage in the water column could foster luxury uptake (i.e., storage of P in algal cells in excess of immediate growth requirements) for later bloom development (Fitzgerald and Nelson 1966). In addition, although storm inflows and P loads were much smaller in late May and June, high SRP concentrations discharged from NW Creek likely subsidized algal growth, as suggested by a mid-June chlorophyll concentration peak. Because the turnover time of P it very rapid (i.e., flux between the dissolved phase and algae is on the order of minutes), any soluble P recycled back to the water column during the crash and decomposition of the June algal bloom could have been immediately assimilated by other successional algal species for growth and later bloom development in August.

Another possible explanation for algal bloom development in late August is direct uptake of hypolimnetic P by vertically-migrating algae. Even though physical entrainment of hypolimnetic available P into the epilimnion was unlikely due to high Fe concentrations, direct P assimilation can be achieved by certain motile algal species (James et al. 1992; Barbiero and Welch 1992; Gervais et al. 2003). For instance, some flagellated species (i.e., *Ceratium hirundinella*, *Gleotrichia echinulata*) can migrate downward through the metalimnion and into SRP gradients for P assimilation (James et al. 1992). Gervais et al. (2003) reported the occurrence of peaks in several phytoplankton species (*Aphanizomenon flos-aquae*, *Planktothrix clathrata*, *Cryptomonas spp.*, *C. hirundinella*, etc) in anoxic, nutrient-rich water located within the metalimnion or upper hypolimnion in Groβer Vätersee. Conversely, certain blue-green algae (i.e., *Aphanizomenon* and *Anabaena* sp.) can reside as cysts or akinites in P-rich sediment and inoculate the water column with surplus supplies of P that can be used for later population increase. By mid-July, hypolimnetic anoxia had extended up to the 3-m depth in Lake Desair and SRP concentration gradients ranged between 0.014 and 0.205 mg/L between the 3- and 4-m depths. An apparent cold front and wind activity in late July resulted in deepening of the epilimnion to about 3 m with very high SRP concentrations occurring at 5-m by mid-August. Thus, SRP concentration gradients extended well into the metalimnion and could have been accessed by motile algal species for uptake. The vertical chlorophyll profile in mid-August exhibited peak concentrations at the 5-m depth in the vicinity of metalimnetic P gradients. Further information is needed to clarify any linkages between vertically-migrating algae, metalimnetic P gradients, and August algal bloom development in Lake Desair. Perhaps samples for algal identification could be collected in 2014 to identify genera occurring in the metalimnion in the summer. Additionally, in situ diel measurements of chlorophyll fluorescence could be measured using recording underwater loggers to detect possible vertical migration by motile algal species.

Empirical modeling suggested that further reduction in NW Creek P loading is needed in order to reduce mean summer chlorophyll concentrations and algal bloom frequency. The model predicted that a 50% reduction in P loading under current 2013 conditions would result in a mean summer chlorophyll concentration of ~ 30 µg/L and a bloom frequency exceeding this mean ~ 50% of the time in the summer. This future condition contrasts with a current chlorophyll mean of 56 µg/L occurring over 70% of the time during the summer. Although much watershed restoration and BMP implementation has occurred in the Lake Desair watershed, more work is needed to identify potential sources and transport of readily dissolved P in the watershed in order to more effectively target reducing the SRP load to the lake (see review by Kleinman et al. 2011). For instance, soils with crop-available P concentrations in excess of crop uptake need may play an important role in desorbing soluble P into the runoff during precipitation events. Analysis of soil P concentration and extractable P in fields that are hydrologically-sensitive to runoff would be useful in identifying critical source areas for management of SRP runoff.

Circulation and artificial destratification has been considered as a lake management tool to reduce algal productivity in Lake Desair by controlling internal P loading (R. Olson, personal commu.). The primary management goal of circulation, artificial destratification, and hypolimnetic aeration is to suppress anoxic P release from sediment by maintaining aerobic conditions and, most importantly, an oxidized environment to minimize Fe reduction, P desorption, and lake accumulation. In the case of Lake Desair, however, the hypolimnetic Fe:P ratio is sufficient to minimize P availability during entrainment events. Even though internal P loading is very high, physical transport of available SRP to the epilimnion is minimal due to oxidation and precipitation. Thus, natural reaeration (i.e., turnover, etc) is probably sufficient to precipitate Fe and P and remove it from biological uptake. Circulation and artificial destratification can also lead to much more rapid heating of the entire lake (as shown for Cedar Lake, WI), stimulating aerobic P mineralization and recycling (Kleeburg et al. 2013). Finally, it can exacerbate dissolved oxygen demand above the sediment interface, leading to continued anoxia, anaerobic reactions, and P release from sediment.

In lieu of the substantial watershed P management needed to meet water quality standards, circulation and artificial destratification may indirectly reduce algal productivity and provide some relief from excess algal blooms by increasing the mixed layer thickness and decreasing the time that algal communities reside in the euphotic zone (i.e., photosynthetically active radiation; Cooke et al. 2005). Maintenance of algal cells below the euphotic zone for a longer period of time could, thus, promote light-limitation of growth (Lorenzen and Mitchell 1975). Additionally, artificial circulation could disrupt vertical migration, the motility of certain algal species, and limit access to hypolimnetic P gradients (Steinberg 1983; Steinberg and Zimmerman 1988). However, little information is available in the literature to substantiate the effectiveness of this approach in controlling algal blooms. In particular, Barbiero et al. (1996) reported that artificial circulation of East Sidney Lake (New York) and changes in $Z_{euphotic\ zone}$:$Z_{mixed\ depth}$ were not important influences of phytoplankton community structure compared to flushing rate, surface temperature, and N:P stoichiometric ratio. Cyanobacteria dominated community structure during the peak growing season in this study. In the case of Lake Desair, an understanding of algal species and motility would shed further light on the possibility of reducing cyanobacterial dominance in August via circulation and artifical destratification.

ACKNOWLEDGMENTS

Desair Lake Restoration, Inc. and the Wisconsin Department of Natural Resources are gratefully acknowledged for financial support of this research. I wish to thank Pamela Toshner and Alex Smith, WI-DNR, for project management and Rod Olsen and Gerry Lisi, Desair Lake Restoration, Inc., for field support, water sampling, and access to boats during the study. I also thank and acknowledge Kirsten Reichman and Jordan Bauer of UW-Stout, Sustainability Sciences Institute, for participating in field sampling and laboratory analytical work.

REFERENCES

Ameel, J.J., Axler, R.P., and Owen, C.J. 1993. Persulfate digestion for determination of total nitrogen and phosphorus in low nutrient water. *American Environmental Laboratory* (October, 1993):8-10.

Amirbahman A, Pearce AR, Bouchard RJ, Norton SQ, Kahl JS. 2003. Relationship between hypolimnetic phosphorus and iron release from eleven lakes in Maine, USA. *Biogeochemistry* 65:369-386.

APHA (American Public Health Association). 2005. Standard Methods for the Examination of Water and Wastewater. 21st ed. Washington (DC).

Barbiero RP, Speziale BJ, Ashby SL. 1996. Phytoplankton community succession in a lake subjected to artificial circulation. *Hydrobiologia* 331:109-120.

Campbell P, Torgersen T. 1980. Maintenance of iron meromixis by iron redeposition in a rapidly flushed monimolimnion. *Can J Fish Aquat Sci* 37:1303–1313.

Caraco NF, Cole JJ, Likens GE. 1989. Evidence for sulphate-controlled phosphorus release from sediments of aquatic systems. *Nature* 341:316–318.

Caraco N, Cole JJ, Likens GE. 1991. A cross-system study of phosphorus release from lake sediments. In (Cole, J., Lovett, G., and Findlay, S., eds.): Comparative analyses of ecosystems: Patterns, mechanisms, and Theories. Springer-Verlag, NY.

Caraco NF, Cole JJ, Likens GE. 1993. Sulfate control of phosphorus availability in lakes. *Hydrobiologia* 253:275-280.

Cedar Corporation. 2006. Desair Lake Restoration, Inc. Lake management activities, August 2003 – May 2006. Cedar Corporation, Menomonie, WI 54751.

Cooke GD, Welch EB, Peterson SA, Nichols SA. 2005. Restoration and management of lakes and reservoirs. 3rd ed. Boca Raton (FL). CRC Press.

Davison W, 1993. Iron and manganese in lakes. *Earth-Science Reviews* 34:119-163.

Davison W, Seed G. 1983. The kinetics of the oxidation of ferrous iron in synthetic and natural waters. *Geochim Cosmochim Acta* 47:67–69.

Fitzgerald GP, Nelson TC. 1966. Extractive and enzymatic analysis for limiting or surplus phosphorus in algae. *J Phycol* 2:32-37.

Gervais F. Siedal U, Heilmann B, Weithoff G, Heisig-Gunkel G, Nicklisch A. 2003. Small-scale vertical distribution of phytoplankton, nutrients and sulphide below the oxycline of a mesoeutrophic lake. *J Plank Res* 25:273-278.

Golterman HL. 1984. Sediments, modifying and equilibrating factors in the chemistry of freshwaters. *Verh int Ver Limnol* 22:23-59.

Golterman HL. 2001. Phosphate release from anoxic sediments or 'what did Mortimer really write? *Hydrobiologia* 450:99-106.

Gunnars A, Blomqvist S. 1997. Phosphate exchange across the sediment–water interface when shifting from anoxic to oxic conditions — an experimental comparison of freshwater and brackish–marine systems. *Biogeochemistry* 37:203–226.
Gunnars A, Blomqvist S, Johansson P, Anderson C. 2002. Formation of Fe(III) oxyhydroxide colloids in freshwater and brackish seawater, with incorporation of phosphate and calcium. *Geochim Cosmochim Acta* 66:745-758.
Hens M, Merckx R. 2002. The role of colloidal particles in the speciation and analysis of “dissolved” phosphorus. *Water Res* 36:1483-1492.
Hoffman AR, Armstrong DE, Lathrop RC. 2013. Influence of phosphorus scavenging by iron in contrasting dimictic lakes. *Can J Fish Aquat Sci* 70:941-952.
Hupfer M, Lewandowski J. 2008. Oxygen controls the phosphorus release from lake sediments – a long-lasting paradigm in limnology. *Int Rev Hydrobiol* 93:415-432.
Idso SB. 1973. On the concept of lake stability. *Limnol Oceanogr* 18:681-683.
James WF, Taylor WD, Barko JW. 1992. Production and vertical migration of Ceratium hirundinella in relation to phosphorus availability in Eau Galle Reservoir, Wisconsin. *Can J Fish Aquat Sci* 49:694-700.
James WF. 2012. Alum dosage considerations for Lake Desair, Wisconsin. University of Wisconsin – Stout, Discovery Center – Sustainability Sciences Institute, 24 October, 2012.
Kleeburg A, Köhler A, Hupfer M. 2012. How effectively does a single or continuous iron supply affect the phosphorus budget of aerated lakes. *J Soil Sediments* 12:1593-1603.
Kleeburg A, Herzog C, Hupfer M. 2013. Redox sensitivity of iron in phosphorus binding does not impede lake restoration. *Water Res* 47:1491-1502.
Kleinman PJA, Sharpley AN, McDowell RW, Flaten DN, Buda AR, Tao L, Bergstrom L, Zhu Q. 2011. Managing agricultural phosphorus for water quality protection: principles for progress. *Plant Soil* 349:169-182.
Lalonde K, Mucci A, Quellet A, Gélinas Y, 2012. Preservation of organic matter in sediments promoted by iron. *Nature* 483:198-200.
Lorenzen MW, Mitchell R. 1975. An evaluation of artificial destratification for control of algal blooms. *J Am Wat Works Assoc* 67:373-376.
Mayer LM, Liotta FP, Norton SA. 1982. Hypolimnetic redox and phosphorus cycling in hypereutrophic Lake Sebasticook, Maine. *Water Res* 16:1189–1196.
Miltenburg JC, Golterman HL. 1988. The energy of the adsorption of o-phosphate onto ferric hydroxide. *Hydrobiologia* 364:93-97.
Mortimer CH. 1941. The exchange of dissolved substances between mud and water in lakes (Parts I and II). *J Ecol* 29:280–329.
Mortimer CH. 1942. The exchange of dissolved substances between mud and water in lakes (Parts III and IV, summary, and references). *J Ecol* 30:147-201.
Mortimer CH. 1971. Chemical exchanges between sediments and water in the Great Lakes – Speculations on probable regulatory mechanisms. *Limnol Oceanogr* 16:387-404.
Nürnberg GK. 1995. Quantifying anoxia in lakes. *Limnol Oceanogr* 40:1100-1111.
Nürnberg GK. 1998. Prediction of annual and seasonal phosphorus concentrations in stratified and polymictic lakes. *Limnol Oceanogr* 43:1544-1552.

Nürnberg GK. 2009. Assessing internal phosphorus load – Problems to be solved. *Lake Reserv Manage* 25:419-432.

Panuska JC, Lillie RA. 1995. Phosphorus loadings from Wisconsin watersheds: Recommended phosphorus export coefficients for agricultural and forested watersheds. Wisconsin Department of Natural Resources Research Management Findings Number 38, April 1995. http://ua.dnr.wi.gov/org/es/science/publications/PUBL_RS_738_95.pdf

Roden EE, Edmonds JW. 1997. Phosphate mobilization in iron-rich anaerobic sewdiments: microbial Fe(III) oxide reduction versus iron sulfide formation. *Arch Hydrobiol* 139:347-378.

Thibault P-J, Rancourt DG, Evans, RJ, Dutrizac JE. 2009. Mineralogical confirmation of a near-P:Fe = 1:2 limiting stoichiometric ratio in colloidal P-bearing ferrihydrite-like hydrous ferric oxide. *Geochim Cosmochim Acta* 73:364–376.

Walker WW. 1996. Simplified procedures for eutrophication assessment and prediction: User manual. Instruction Report W-96-2, September, 1996, U.S. Army Engineer Waterways Experiment Station, Vicksburg, Mississippi, USA.

Wauer G, Gonsiorczyk T, Hupfer M, Koschel R. 2009. Phosphorus balance of Lake Tiefwarensee during and after restoration by hypolimnetic treatment with aluminum and calcium salts. *Lake Reserv Manage* 25:377-388.

Welschmeyer NA. 1994. Fluorometric analysis of chlorophyll a in the presence of chlorophyll b and pheaopigments. *Limnol Oceanogr* 39:1985-1992.

Table 1. Physical characteristics for Lake Desair and it's watershed.

Feature	Characteristic	Value			
Watershed	Total area	1,527	ha	3773	ac
Lake	Surface area	321,114	m^2	80	ac
	Volume	1,634,421	m^3	1350	ac-ft
	Mean depth	5.1	m	16.7	ft
	Maximum depth	10.1	m	33	ft
	Maximum fetch	1.3	km	0.8	mi
	Osgood index	9.0			

Table 2. Mean annual (2013) hydrological characteristics.

Variable	Value			
Annual precipitation	0.85	(m)	33.61	(inches)
NW Creek mean daily flow	0.055	(m^3/s)	1.96	(ft^3/s)
NW Creek annual water income	1.75	(Hm^3/y)	1419	(acre-ft)
NW Creek areal water load	5.4	(m/y)	17.7	(ft/y)
Theoretical residence time	0.93	(y)		
Flushing rate	1.07	(y^{-1})		

Table 3. Estimated total and soluble phosphorus (P) mass loading and mean flow-weight concentration for the NW Creek draining into Lake Desair.

Time period	Total P			Soluble P			
	(kg)	(lbs)	(mg//L)	(kg)	(lbs)	(mg//L)	(% TP)
Summer[1]	19	43	0.246	5	12	0.066	27
Annual	755	1664	0.431	276	608	0.158	37

[1]1 June to 30 September

Table 4. Mean (MAY-SEP) total phosphorus (TP), chlorophyll (CHL), Secchi transparancy (SD), and Trophic State Index (TSI; Carlson 1977) for the upper 1-m water column of Lake Desair.

Variable	Value
Total P (mg/L)	0.078
Chlorophyll (ug/L)	56
Secchi transparency (m)	0.9
TSI-TP	66
TSI-CHL	67
TSI-SD	62

Table 5. Phosphorus (P) mass balance used to estimate summer net internal P loading in Lake Desair. Please see equation 4 in Methods for term definitions.

P Flux	5/21/13 to 9/9/13 (111 Days)	
	(kg)	(mg/m^2 d)
$P_{lake\ storage}$	362	10.2
$P_{external\ load}$	19	0.5
$P_{outflow}$	6	0.2
$P_{net\ retention}$	13	0.4
$P_{net\ internal\ load}$	-349	-9.8

Table 6. Various estimates of internal phosphorus (P) loading for Lake Desair.

Estimate	Internal P load estimate	kg/y	mg/m2 d
1	Gross internal P loading from Nurnberg (1998) empirical model	436	12.2
2	Net internal P loading from summer P budget (Table 5)	349	9.8
3	Gross internal P loading from P release rates and anoxic factor[1]	300	9.8
	Mean internal P load	362	10.6

James (2012)

Table 7. Algorithms used for Bathtub (Walker 1996) phosphorus loading reduction modeling.

Variable	Model
Phosphorus	Walker available P
Chlorophyll	Jones and Bachmann
Secchi Transparency	versus Chlorophyll & Turbidity

Table 8. Predicted lake response to Northwest (NW) Creek phosphorus (P) loading reduction from current (2013) conditions.

NW Creek P load reduction	Predicted Lake Total Phosphorus		Predicted Lake Chlorophyll		Predicted Lake Secchi Transparency	
(% of current conditions)	(mg/L)	(% reduction)	(ug/L)	(% reduction)	(m)	(% increase)
Current	0.087	0	55	0	0.90	0
90	0.082	6	51	8	1.00	5
80	0.077	12	46	16	1.05	10
70	0.071	18	41	25	1.10	16
60	0.066	25	36	34	1.15	24
50	0.059	32	31	43	1.20	32
40	0.052	40	26	53	1.30	43
30	0.044	49	21	63	1.40	56
20	0.035	60	15	74	1.60	73

Table 9. Predicted bloom frequency to Northwest (NW) Creek phosphorus (P) loading reduction from current (2013) conditions. Red values denote example bloom frequencies as discussed in the Results and Discussion section.

NW Creek P load reduction	Predicted frequency that the below chlorophyll concentration is exceeded during the summer growing season (%)					
(% of current conditions)	> 10 ug/L	> 20 ug/L	> 30 ug/L	> 40 ug/L	> 50 ug/L	> 60 ug/L
Current	99.3	90.7	**74.7**	58.0	43.7	32.6
90	98.9	88.2	70.2	52.6	38.4	27.8
80	98.4	84.9	64.7	46.5	32.7	22.9
70	97.6	80.4	58.0	39.7	26.7	18.0
60	96.2	74.4	50.0	32.1	20.5	13.2
50	93.7	66.1	**40.5**	24.1	14.4	8.7
40	89.2	54.6	29.5	15.8	8.7	4.9
30	80.2	39.3	17.8	8.3	4.0	2.1
20	61.7	20.6	7.0	2.6	1.1	0.5
10	25.6	3.8	0.8	0.2	0.1	0.0

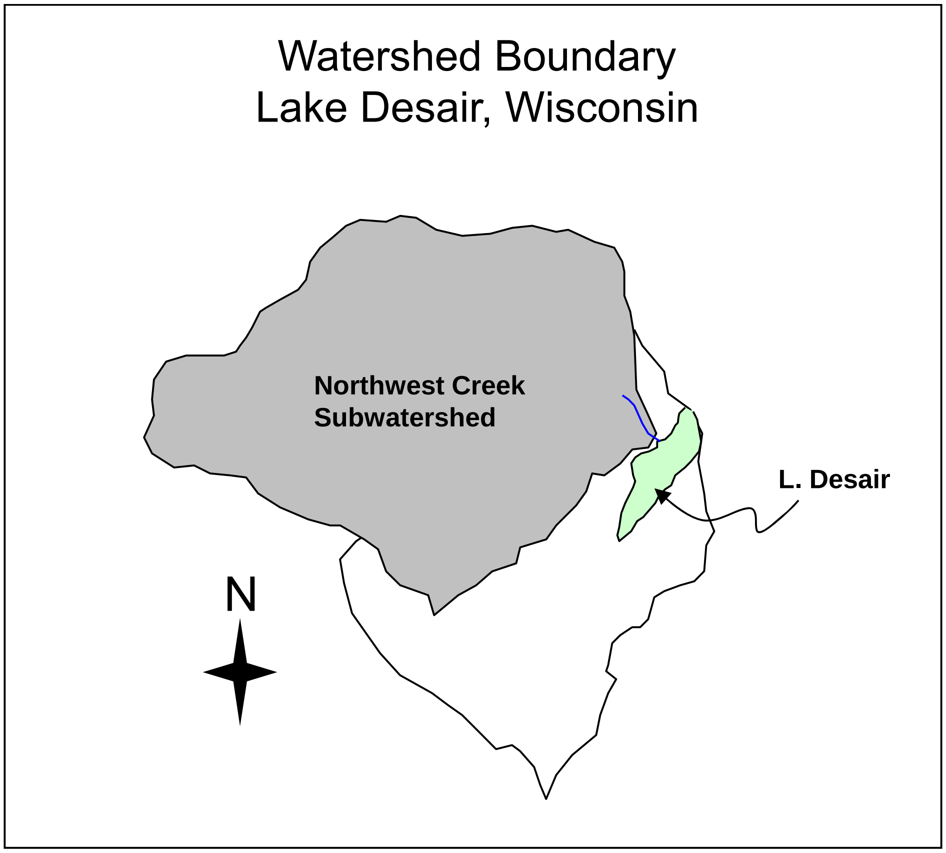

Figure 1. Catchment area for Lake Desair and the Northwest Creek subwatershed.

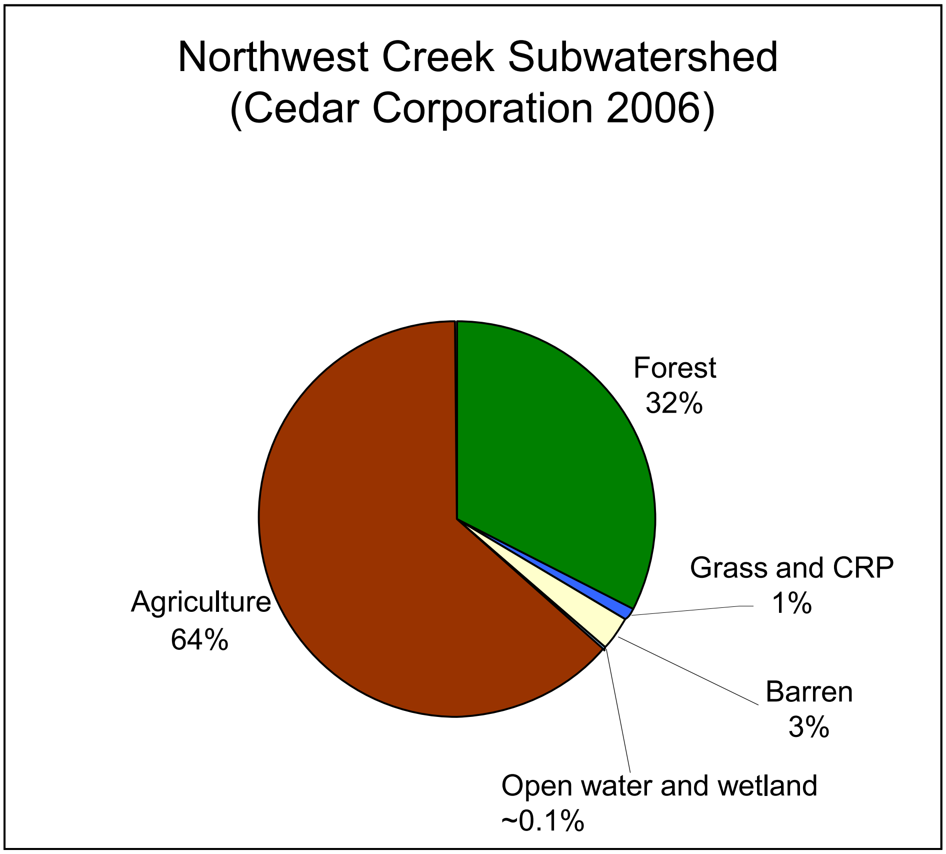

Figure 2. Percentages of various land-use practices in the Northwest Creek subwatershed.

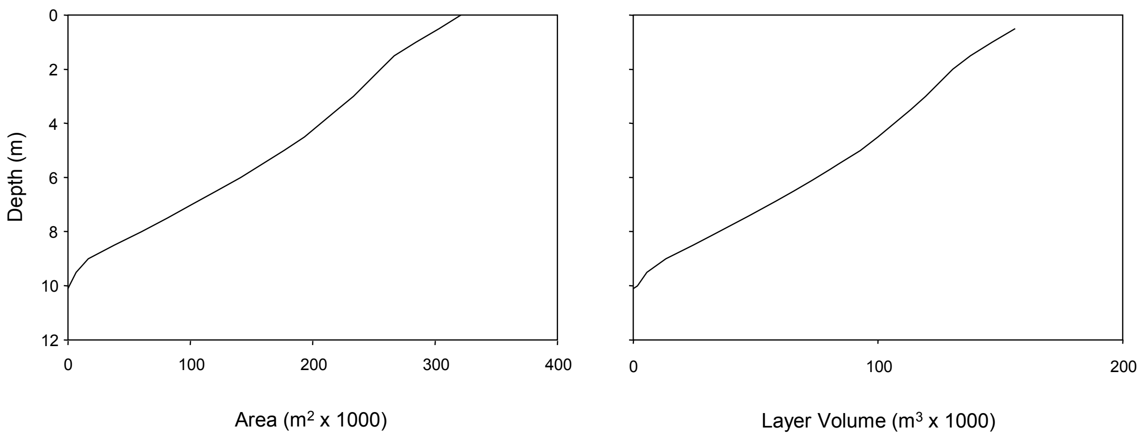

Figure 3. Lake Desair hypsograph showing area and volume characteristics.

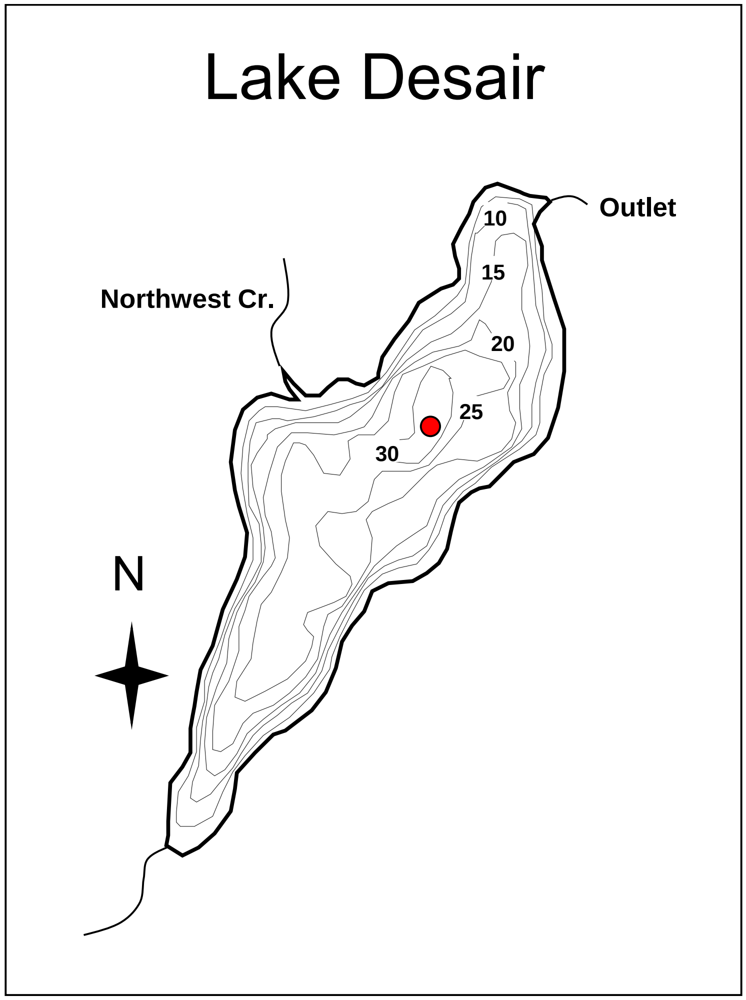

Figure 4. Bathymetric map of Lake Desair. Red circle denotes the location of the limnological sampling station.

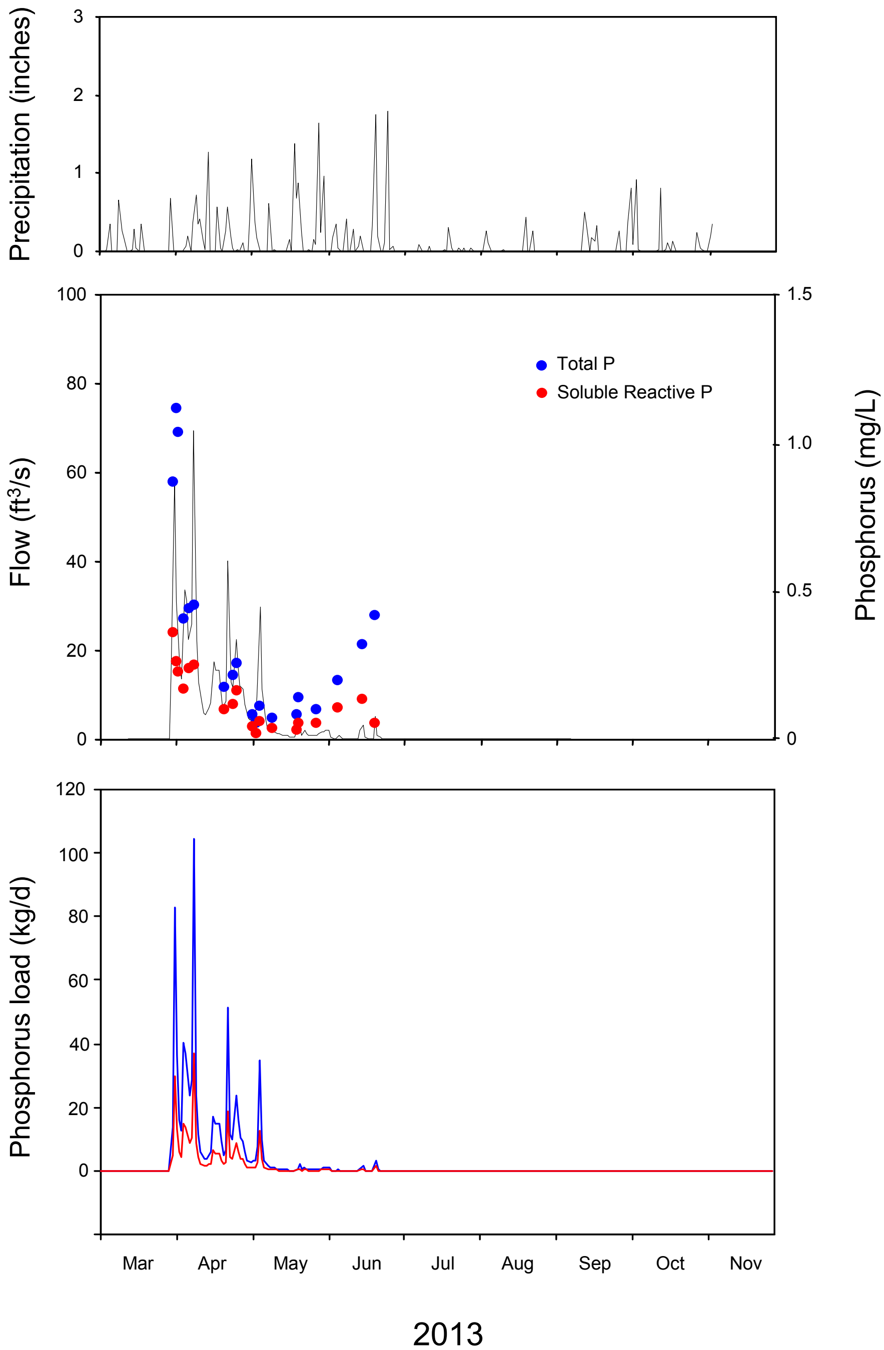

Figure 5. Time series of daily precipitation (upper panel), Northwest Creek mean daily discharge with concentrations of total and soluble reactive phosphorus (P; middle panel), and daily total and soluble reactive P loading from Northwest Creek (lower panel).

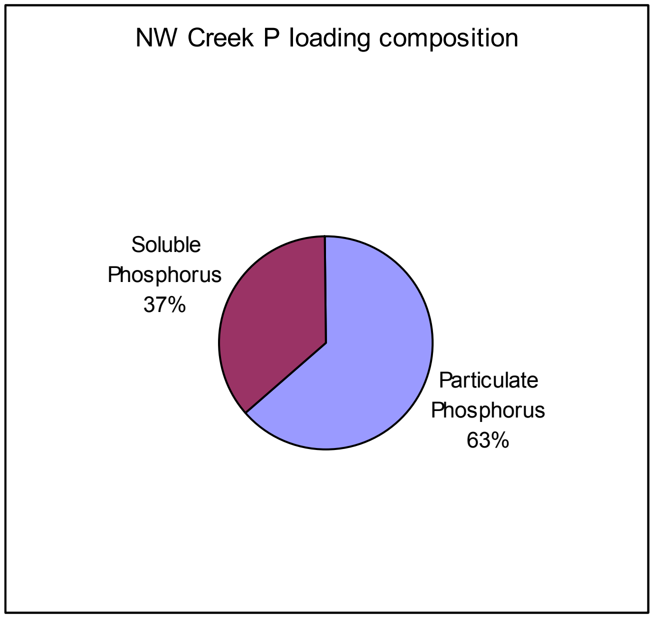

Figure 6. Composition of the Northwest (NW) Creek annual total phosphorus (P) load.

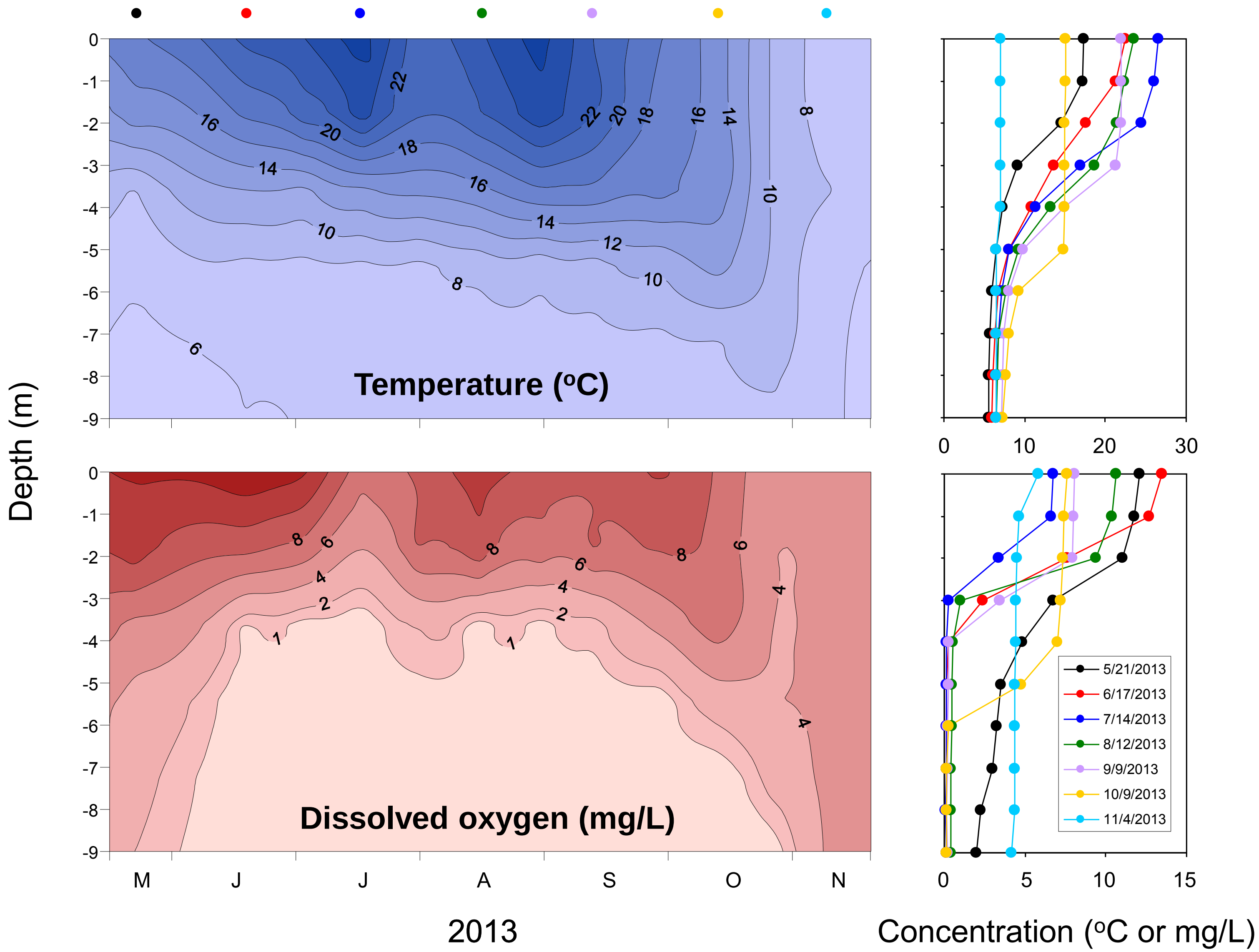

Figure 7. Seasonal and vertical variations in temperature (upper panel) and dissolved oxygen (lower panel) in Lake Desair.

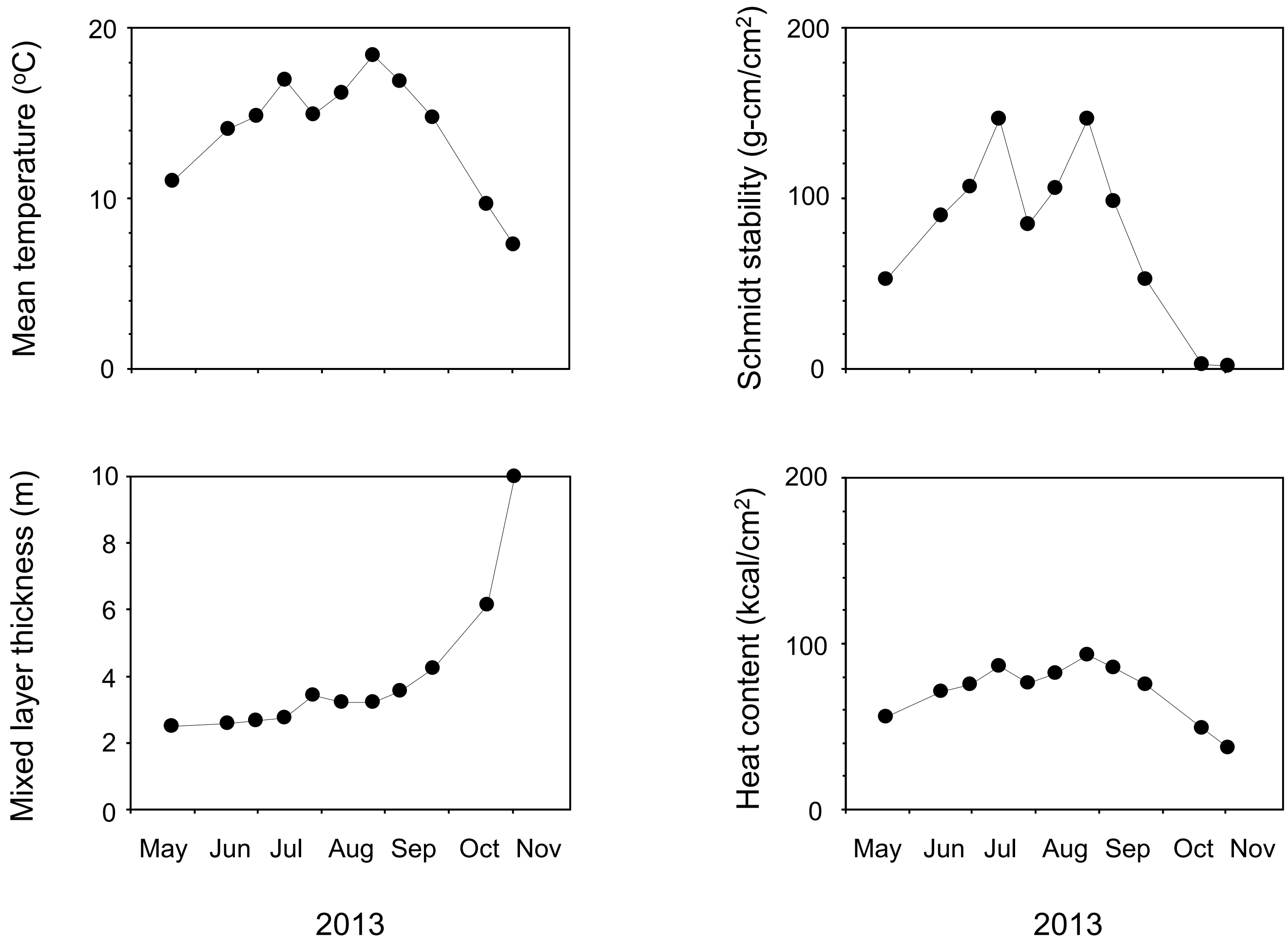

Figure 8. Seasonal variations in mean lake temperature (upper left), the mixed layer depth (epilimnion; lower left), Schmidt stability (upper right), and heat content (lower right) for Lake Desair.

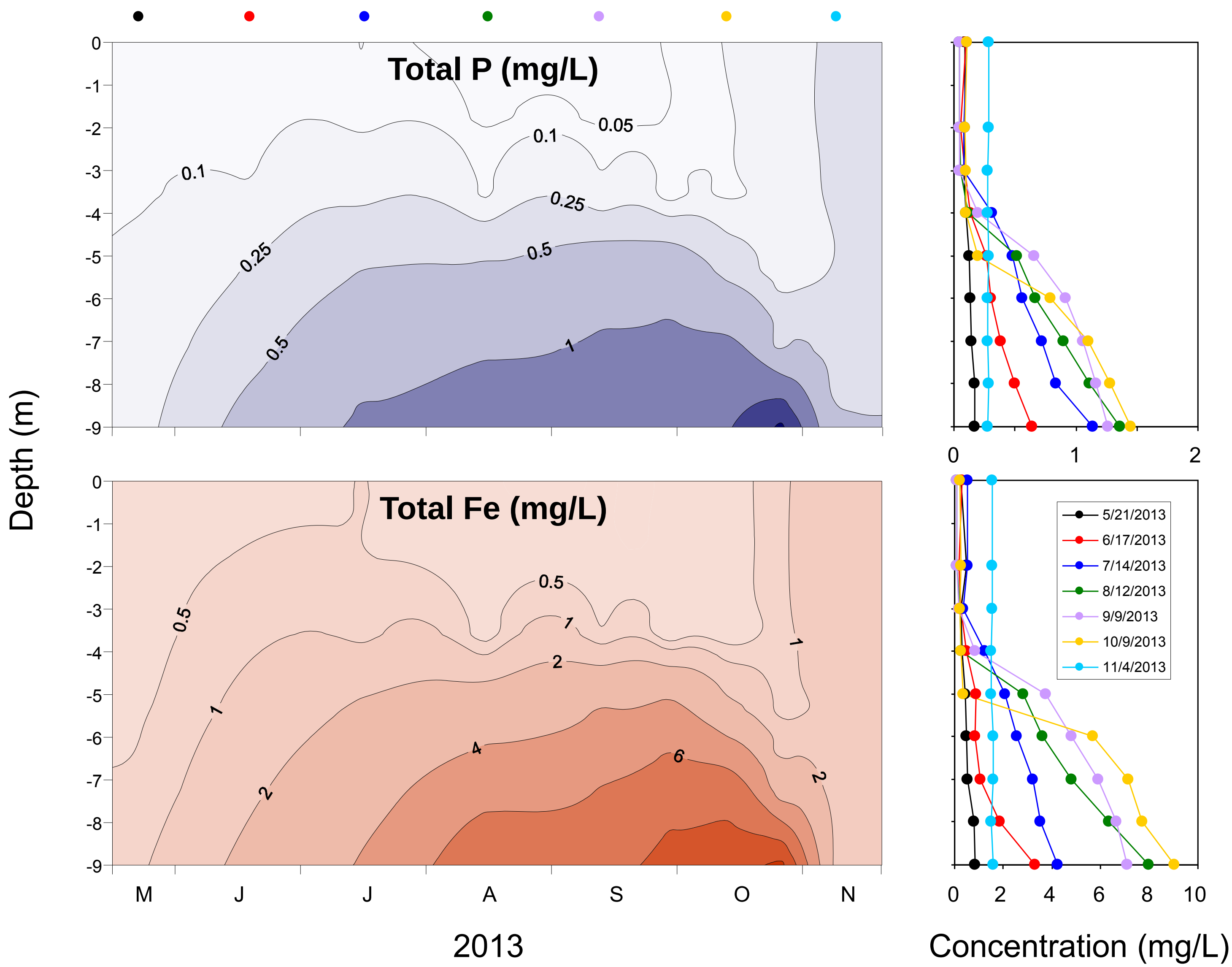

Figure 9. Seasonal and vertical variations in total phosphorus (P; upper panel) and total iron (Fe; lower panel) in Lake Desair.

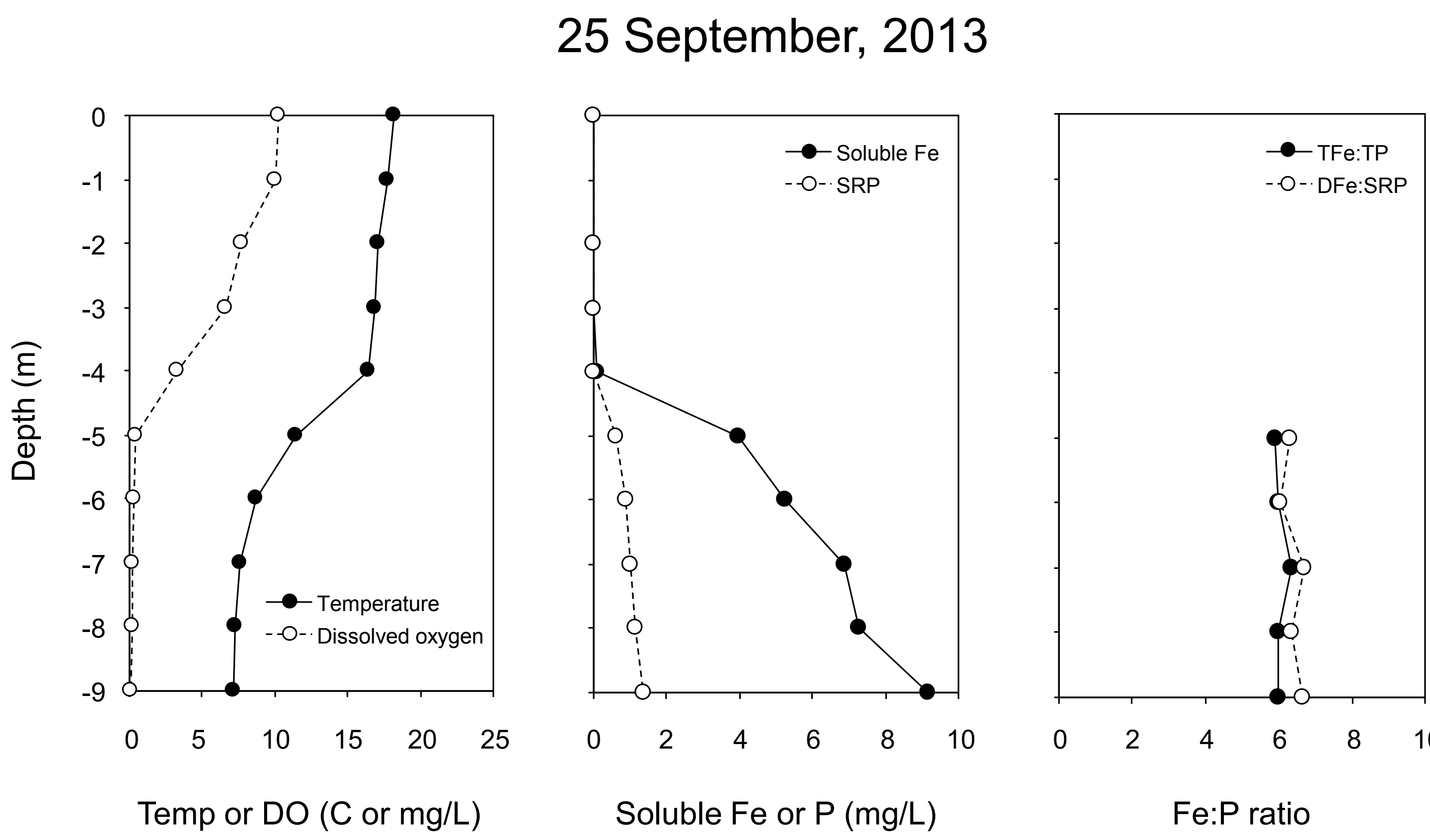

Figure 10. Vertical profiles of temperature and dissolved oxygen (left), soluble iron (Fe) and phosphorus (P; center), and the hypolimnetic iron to phosphorus ratio (TFe:TP = total Fe:total P ratio; DFe:SRP = dissolved Fe:soluble reactive P ratio) on 23 September, 2013.

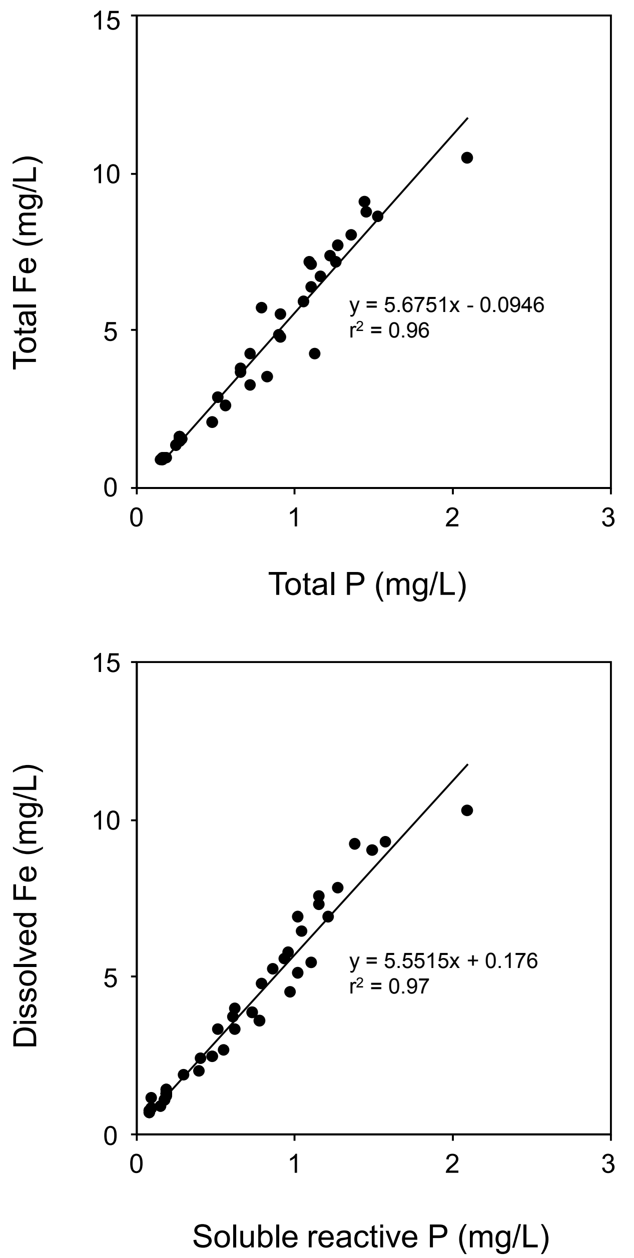

Figure 11. Linear relationships between hypolimnetic total iron (Fe) and total phosphorus (P; upper panel) and dissolved Fe and and soluble reactive P (lower panel). The slope of each regression equation (i.e., 5.67 and 5.55) approximates the Fe:P ratio. An Fe:P ratio (mass:mass) greater than 3.6:1 indicates complete adsorption of PO_4^{3-} *to iron oxyhydroxides after chemical oxidation of Fe during fall turnover. For instance, at least 4 parts of oxidized iron are required to completely bind 1 part of phosphate.*

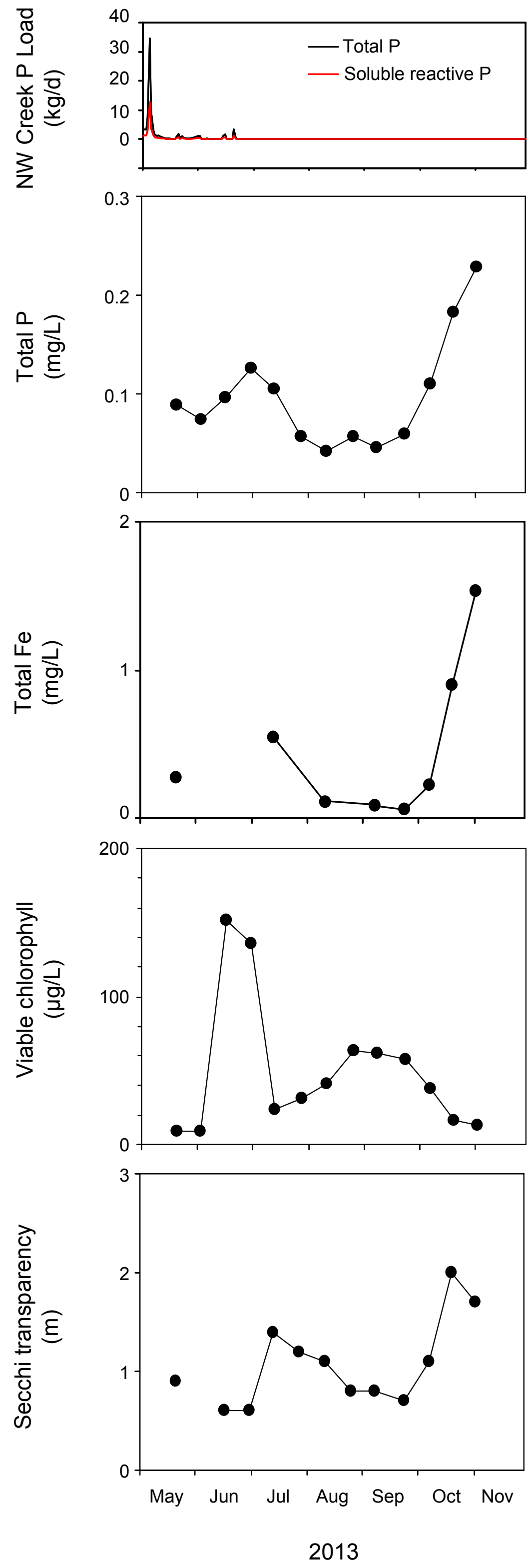

Figure 12. Seasonal variations in the Northwest (NW) Creek total and soluble reactive phosphorus (P) load, concentrations of total P, total iron (Fe), and chlorophyll in the upper 1-m water column, and Secchi transparency in Lake Desair during 2013.

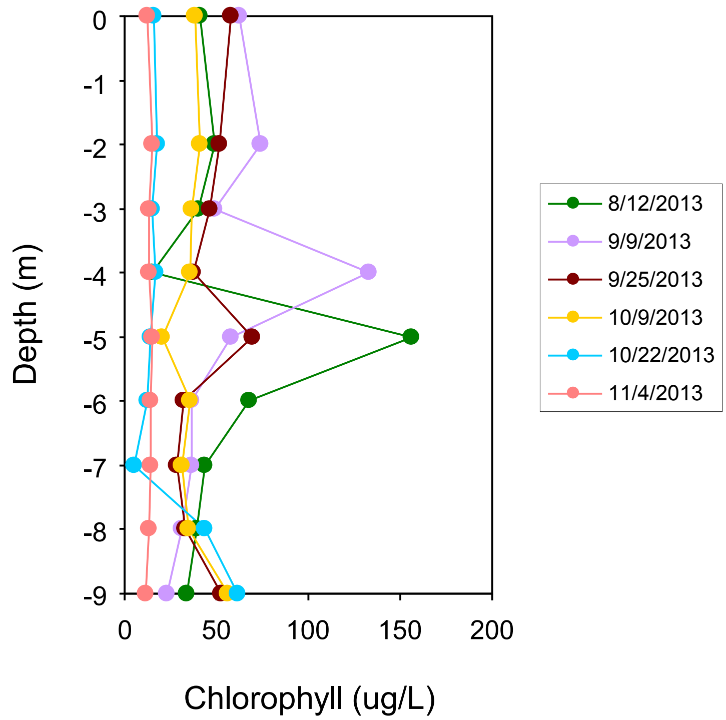

Figure 13. Vertical variations in viable chlorophyll in Lake Desair between mid-August and early November, 2013.

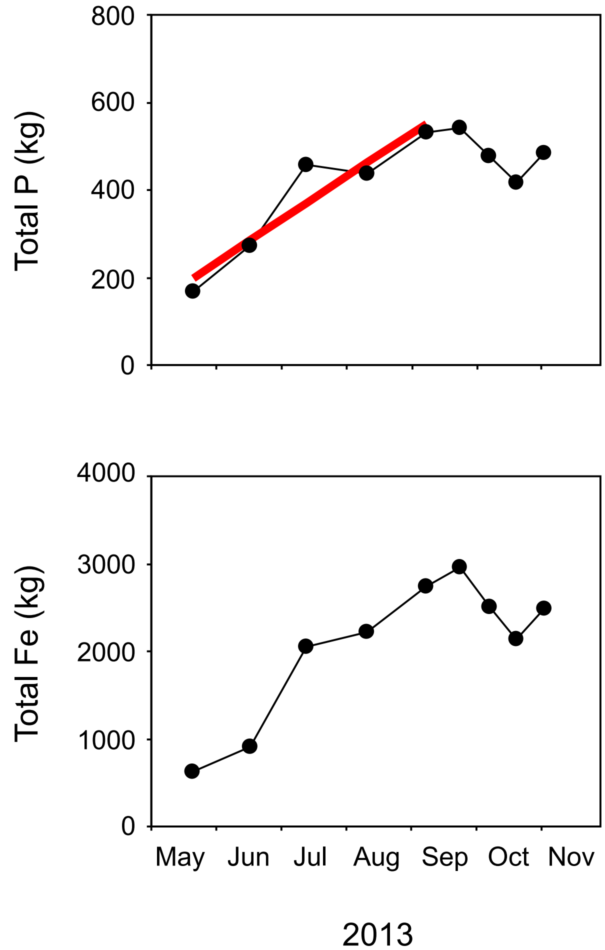

Figure 14. Seasonal variations in estimated total phosphorus (P; upper panel) and total iron (Fe; lower panel) mass in Lake Desair in 2013. Red bar denotes the time period used to estimate net internal phosphorus loading in the lake.

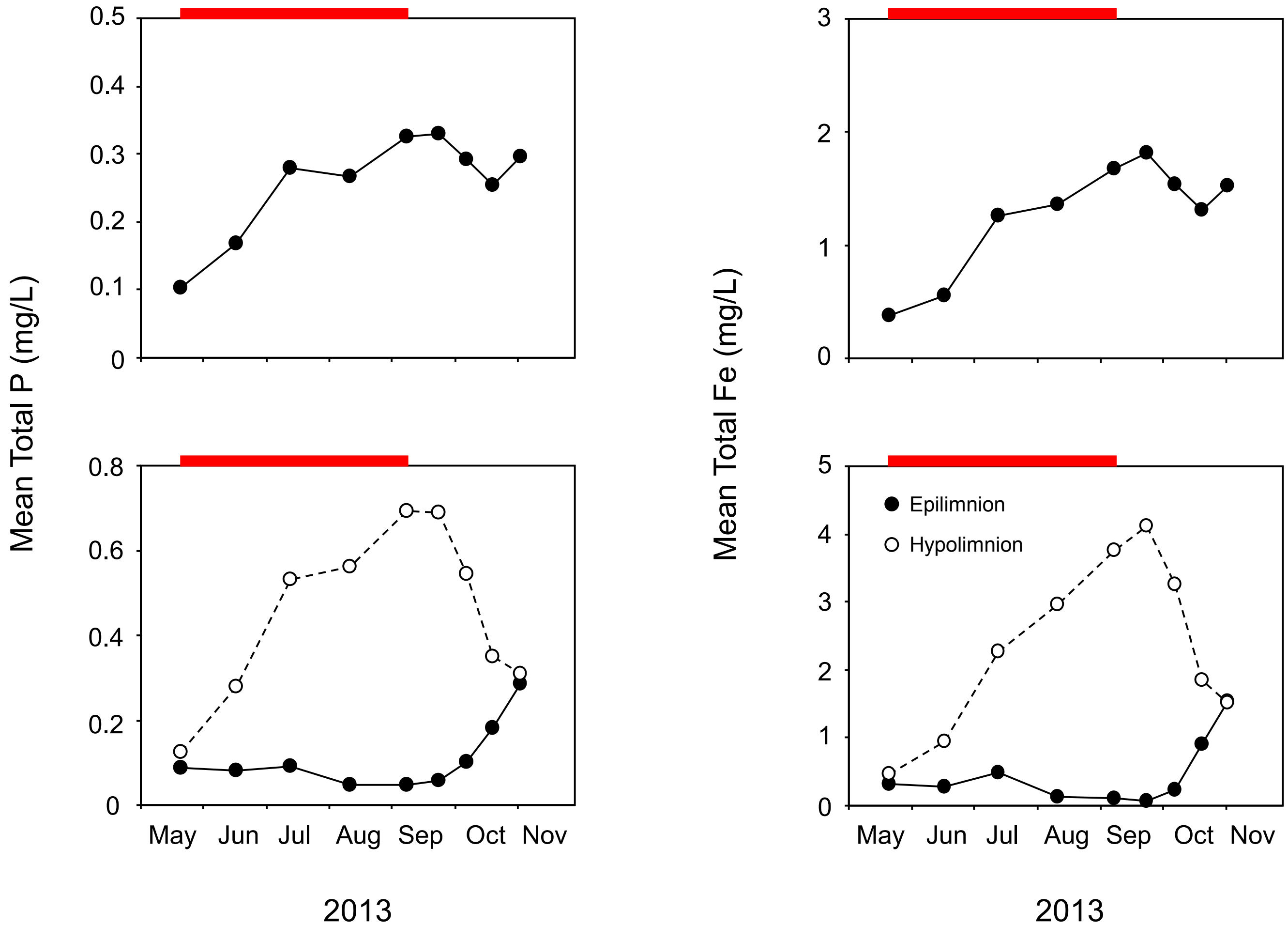

Figure 15. Seasonal variations in mean water column total phosphorus (P; upper left panel) and total iron (Fe; upper right panel) and mean concentrations in the epilimnion and hypolimnion (lower panels). Red bar denotes the time period used to estimate net internal phosphorus loading in the lake.

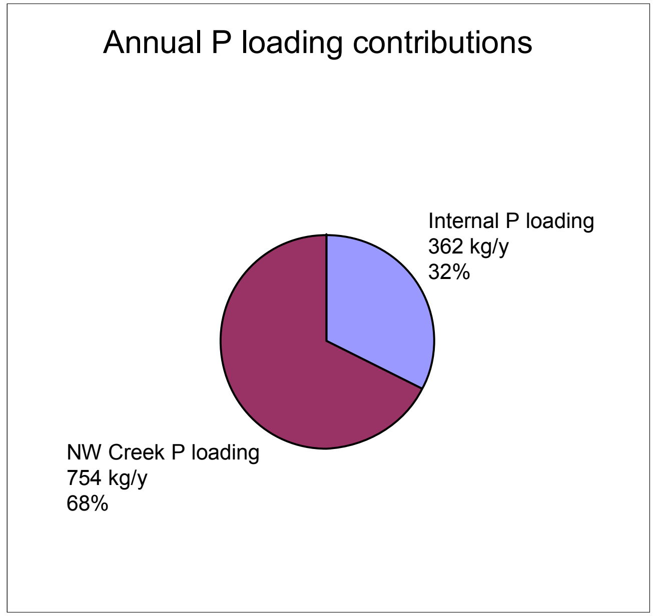

Figure 16. Contribution of Northwest (NW) Creek and internal phosphorus (P) loads to the measured annual P budget of Lake Desair.

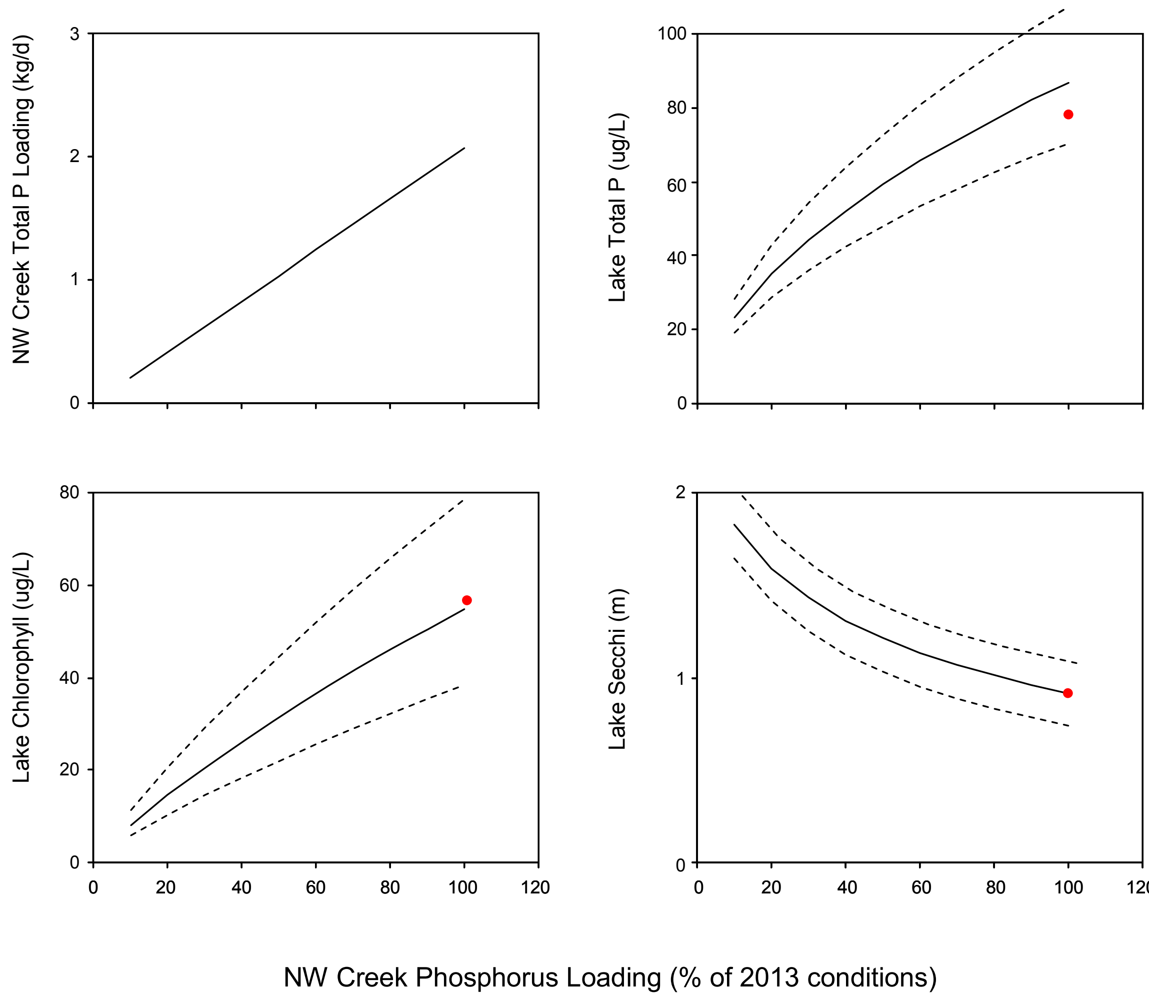

Figure 17. Bathtub (Walker 1996) model output of predicted changes in total phosphorus (P), chlorophyll, and Secchi transparency in Lake Desair as a function of reducing Northwest (NW) Creek tributary P loading from 2013 leve s(black lines). Dotted lines denote 95% confidence intervals. Red circles represent current measured mean values (see Table 4).

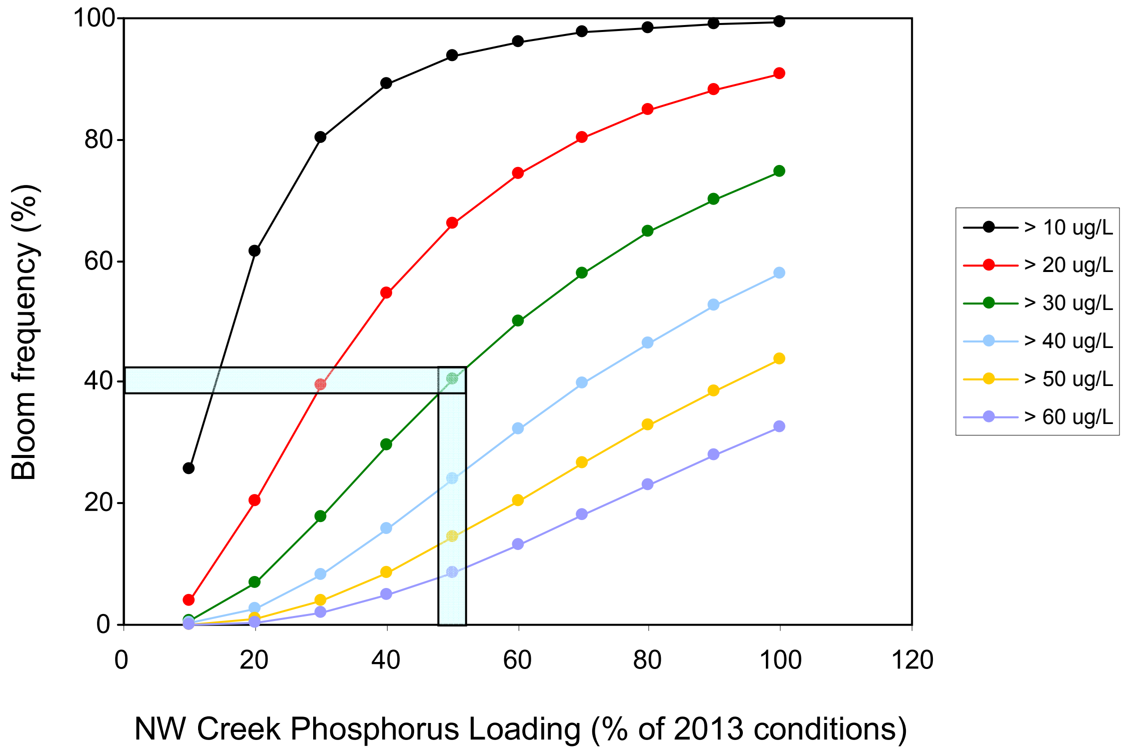

Figure 18. Bathtub (Walker 1996) model output of predicted changes in algal bloom frequency (as chlorophyll) as a function of decreases in 2013 Northwest (NW) Creek tributary phosphorus (P) loading from 2013 levels. The light blue shaded area highlights predicted changes in the frequency of blooms greater than 30 µg/L after a 50% reduction in NW Creek P loading.